Atmos. Chem. Phys., 11, 9971–9982, 2011
www.atmos-chem-phys.net/11/9971/2011/
doi:10.5194/acp-11-9971-2011

Atmospheric Chemistry and Physics

Modeling interfacial liquid layers on environmental ices

M. H. Kuo, S. G. Moussa, and V. F. McNeill

Department of Chemical Engineering, Columbia University, New York, New York 10027, USA

Received: 8 February 2011 – Published in Atmos. Chem. Phys. Discuss.: 10 March 2011
Revised: 12 September 2011 – Accepted: 12 September 2011 – Published: 28 September 2011

Abstract. Interfacial layers on ice significantly influence air-ice chemical interactions. In solute-containing aqueous systems, a liquid brine may form upon freezing due to the exclusion of impurities from the ice crystal lattice coupled with freezing point depression in the concentrated brine. The brine may be segregated to the air-ice interface where it creates a surface layer, in micropockets, or at grain boundaries or triple junctions.

We present a model for brines and their associated liquid layers in environmental ice systems that is valid over a wide range of temperatures and solute concentrations. The model is derived from fundamental equlibrium thermodynamics and takes into account nonideal solution behavior in the brine, partitioning of the solute into the ice matrix, and equilibration between the brine and the gas phase for volatile solutes. We find that these phenomena are important to consider when modeling brines in environmental ices, especially at low temperatures. We demonstrate its application for environmentally important volatile and nonvolatile solutes including NaCl, HCl, and HNO_3. The model is compared to existing models and experimental data from literature where available. We also identify environmentally relevant regimes where brine is not predicted to exist, but the QLL may significantly impact air-ice chemical interactions. This model can be used to improve the representation of air-ice chemical interactions in polar atmospheric chemistry models.

1 Introduction

Ice-gas interactions in the environment affect atmospheric composition and climate in a number of ways. Exchange of trace gases with snowpack and frozen halide surfaces largely control atmospheric composition in polar regions (Domine and Shepson, 2002; Grannas et al., 2007a; Simpson et al., 2007).The heterogeneous chemistry of cloud ice particles also plays critical roles in polar stratospheric ozone depletion (Solomon et al., 1986; Molina et al., 1987; McNeill et al., 2006), in tropospheric chemistry (McConnell et al., 1992; von Kuhlmann and Lawrence, 2006; Gamblin et al., 2006, 2007), and in climate (Gao et al., 2004). A quantitative physical understanding of the interactions of snow and ice with trace gases is critical for atmospheric chemistry modeling, as well as for the interpretation of records of climate and biogeochemistry obtained via ice core analysis (Domine and Shepson, 2002). Furthermore, the extent of snow and ice ground cover, sea ice, and cloud ice particle numbers are sensitive to changes in global climate (Lemke et al., 2007; Anisimov et al., 2007; Denman et al., 2007). Therefore, accurate representation of the heterogeneous chemistry of snow and ice in coupled atmospheric chemistry-Earth system models is necessary in order to predict the effects of climate change on atmospheric composition.

Interfacial layers on ice contribute to the reactivity of ice surfaces and their ability to catalyze chemical reactions. Interfacial layers on ice and snow can be categorized into two conceptually distinct regimes: the “quasi-liquid layer’ (QLL), and brine layers (BL). The QLL is a nanoscale region of surface disorder that exists on pure ice (or at very low impurity concentrations) below the melting temperature. It is not a true liquid phase: it violates Gibbs’ Phase Rule. In contrast, brines are true liquids that exist in equilibrium with pure ice in frozen aqueous systems with higher solute content (e.g. sea ice, or snow with contaminants) (Cho et al., 2002; Wettlaufer et al., 1997). Brines form when water containing solutes is frozen and impurities are excluded from the ice lattice, resulting in their selective segregation and concentration at the crystal surface, grain boundaries, micropockets, or triple junctions (Harrison and Raymond, 1976; Maccagnan and Duval, 1982c; Takenaka and Bandow, 2007; Takenaka et

Correspondence to: V. F. McNeill
(vfm2103@columbia.edu)

al., 1992, 1996; Robinson et al., 2006; Mulvaney et al., 1988; Fukazawa et al., 1998; Baker et al., 2003, 2007; Cullen and Baker, 2000; Wolff et al., 1989; Huthwelker et al., 2001). Acids are believed to concentrate at the grain boundaries and triple junctions in glacier ice and polar ice sheets, existing in an aqueous brine (Harrison and Raymond, 1976; Maccagnan and Duval, 1982; Wolff and Paren, 1984; Mulvaney et al., 1988; Fukazawa et al., 1998; Baker et al., 2003, 2007; Cullen and Baker, 2000; Wolff et al., 1989; Huthwelker et al., 2001; Bartels-Rausch et al., 2004) The segregation effect is coupled with freezing point depression in the brine as it becomes more concentrated. Freeze concentration can create pH changes in the brine and accelerate aqueous chemistry (Takenaka and Bandow, 2007; Takenaka et al., 1992, 1996; Grannas et al., 2007b).

Brine on snow and ice is typically represented in snow chemistry models using a thermodynamic model which assumes ideal solution behavior in the brine based on a fixed input solute content (Cho et al., 2002; Boxe and Saiz-Lopez, 2008), or by assuming a constant brine volume fraction or layer thickness (Michalowski et al., 2000; Liao and Tan, 2008; Thomas et al., 2011). Existing models assume complete exclusion of impurities from the ice lattice, whereas some environmentally important solutes have been shown to have small but non-negligible solubility in the ice matrix (Thibert and Domine, 1997, 1998). It is also generally assumed that equilibration of solutes with the gas phase when the brine is in equilibrium with surface air or firn air does not influence brine thickness.

In this study we present a model for brines and their associated liquid layers on environmental ices. The unique aspects of this model are that it takes into account nonideal solution behavior in the concentrated brine, partitioning of the solute into the ice matrix, and equilibration between the brine and the gas phase for volatile solutes. We demonstrate its application to volatile and non volatile environmentally relative solutes such as NaCl, HCl, and HNO_3 and compare its performance to existing models and experimental data where available. We find that accounting for nonideal solution behavior in the concentrated brine and partitioning of the solute into the ice matrix is particularly important for modeling brines in environmental ices at low temperatures. We also identify environmentally relevant concentration and temperature regimes where brine is not predicted to exist based on these models, but the QLL may affect significantly air-ice chemical interactions.

2 Modeling approach

A general description of the model is followed by more specific discussions on the treatment of (1) non-volatile solutes and (2) soluble gas-phase strong acids. All the symbols used in this section are defined in Appendix A.

2.1 General description of the brine model

For a brine existing in equilibrium with ice, the mole fraction and activity coefficient of the solute in the brine are related to system temperature and pressure by the following thermodynamic relationship:

$$\frac{1}{1-x_s}\left[x_s\left(\frac{\partial \ln\gamma_s}{\partial x_s}\right)_{T,P}+1\right]\frac{dx_s}{dT}=\frac{-\Delta H_w^{fus}}{RT^2} \quad (1)$$

where x_s is the mole fraction of solute in the brine, γ_s is the activity coefficient of the solute in the brine, ΔH_w^{fus} is the enthalpy of fusion of water, R is the gas constant, T and P are the system temperature and pressure. The details of the derivation of Eq. (1) are presented in the Supplement. For ideal solution behavior in the brine, the term $x_s\left(\frac{\partial \ln\gamma_s}{\partial x_s}\right)_{T,P}$ in Eq. (1) goes to zero. This term can be regarded as a measure of the deviation from ideality, and is referred to as the "non-ideality index" hereinafter in this work. For the ideal solution case (non-ideality index $\rightarrow 0$) an analytical solution to Eq. (1), similar to that presented by Cho et al. (2002), can be obtained and is given by

$$x_s = 1-(1-x_{s,0})\exp\left[\frac{-\Delta H_w^{fus}}{R}\left(\frac{1}{T}-\frac{1}{T_m}\right)\right] \quad (2)$$

where $x_{s,0}$ is the mole fraction of the solute in the completely melted sample and T_m is the bulk melting temperature of ice.

Using expressions of γ_s available in the literature, Eq. (1) can be solved numerically for x_s and the non-ideality index can be evaluated. Parameterized equations of activity coefficients as functions of temperature and solute concentration are available in the literature for various substances (Akinfiev et al., 2001; Carslaw et al., 1995; Clegg and Brimblecombe, 1990; Massucci et al., 1999).

The predicted solute mole fraction in the brine, x_s, can be used to calculate the fraction of moles in the brine layer, φ:

$$\varphi = \frac{n_s^{brine}+n_w^{brine}}{n_s+n_w}\left(\frac{n_s}{n_s^{brine}}\right)=\frac{x_{s,0}}{x_s} \quad (3)$$

where n_s^{brine} and n_w^{brine} are the moles of solute and water in the brine, respectively, and n_w and n_s are the amount of water and solute in the total sample, respectively. For solutes such as HCl and HNO_3 which may partition to the ice matrix (Thibert and Domine, 1997, 1998), the amount of solute in the ice is equal to $\left(n_s-n_s^{brine}\right)$ otherwise if the solute is completely sequestered in the brine, $n_s=n_s^{brine}$. Brine mole fraction is related to brine volume fraction, φ_V, via the densities (ρ_i) and molar masses (M_i) of the brine and the total sample:

$$\varphi_V=\varphi\left(\frac{M_{brine}}{\rho_{brine}}\right)\left(\frac{\rho_{total}}{M_{total}}\right) \quad (4)$$

Note that M_i (i = brine or total) and ρ_{total} are mole-fraction-weighted averages. The brine density can be estimated

from density correlations, such as those given in Clegg and Wexler (2011) for many environmentally relevant solutions.

In the absence of brine micropockets, a simple geometric argument allows us to estimate the thickness of the brine layer from the volume fraction.

$$d_{\mathrm{BL}}=\varphi_V\left(\frac{V}{A}\right) \tag{5}$$

where V/A is the volume to surface area ratio of the ice sample. V/A can be flexibly adjusted to describe the geometric characteristics of the system of interest. Therefore, this treatment can be applied to grain boundaries as well as at the gas-ice interface, provided that a reasonable representation of grain shape and size is available. Thomas et al. (2011) assumed spherical grains with $r = 1$ mm radius in their snow model, in this case $d_{\mathrm{BL}} = (r/3)\varphi_V$.

Note that the model described by Eqs. (1–5) yields a liquid layer thickness of zero at zero impurity concentration (even at temperatures close to the melting point) and therefore will not predict the presence of the QLL on pure ice in the absence of solute. In the next few paragraphs, we discuss more specifically about how the modeling method described by Eqs. (1–5) can be adapted to (1) systems with non-volatile solutes and (2) systems with volatile solutes which exist in equilibrium between the gas phase, the brine, and the ice matrix (e.g. HNO_3 and HCl).

2.2 Non-volatile solutes

For systems containing only non-volatile solutes, the solute concentration in the melt is generally known and fixed, making the solution of Eq. (1) or Eq. (2) straightforward. We show an application to the NaCl-H_2O system in Sect. 3.1. Note that for non-volatile solutes the concentration and activity coefficient equations are often expressed in terms of molality rather than mole fraction. Equation (1) written in terms of solute molality can be found in the Supplement.

2.3 Volatile solutes

Volatile solutes exist in equilibrium between the brine and any adjacent gas phase (i.e. firn or surface air) according to Henry's Law. For a generic gas phase acidic species HA, which dissociates completely in solution to form H^+ and A^- (Carslaw et al., 1995):

$$p_{\mathrm{HA}}=\frac{1}{K_H}x_{\mathrm{H}}\gamma_{\mathrm{H}}x_{\mathrm{A}}\gamma_{\mathrm{A}}=\frac{1}{K_H}x_{\mathrm{H}}x_{\mathrm{A}}\gamma_{\pm} \tag{6}$$

where p_{HA} is the partial pressure of HA, K_H is the Henry's law constant, x_i and γ_i are the mole fraction and activity coefficient of ion i, and $\gamma_\pm$ is the mean ionic activity coefficient. Henry's law constants expressed as functions of temperature have been determined for a number of atmospherically important species (Carslaw et al., 1995; Clegg and Brimblecombe, 1990; Massucci et al., 1999).

Some volatile solutes are also known to diffuse into the ice matrix. Knowing the partial pressure, the mole fraction of gas dissolved into the ice phase has been determined to follow the relationship (Thibert and Domine, 1997, 1998):

$$x_{\mathrm{s}}^{\mathrm{ice}}=A_0\exp\left(\frac{\Delta h_{\mathrm{s}}^{\mathrm{sub}}}{RT}\right)(p_{\mathrm{s}})^{1/n} \tag{7}$$

where $x_{\mathrm{s}}^{\mathrm{ice}}$ is the equilibrium mole fraction of solute "s" in ice, A_0 is a constant, $\Delta h_{\mathrm{s}}^{\mathrm{sub}}$ is the partial molar enthalpy of sublimation of "s" from ice, p_{s} is the partial pressure of the solute in the gas, and n is the ice vapor pressure depression factor.

When modeling the volume fraction or layer thickness in a system where such processes are involved, two scenarios naturally arise. The first scenario is one in which the concentration of dissolved species in the melt sample is known. This is akin to field studies where snow samples are collected and melted for analysis. In the second scenario the partial pressure of the solute gas is known, but partitioning to the condensed phase is unknown, as is the case in typical laboratory uptake experiments. Although the general modeling framework remains the same (Eqs. 1–5), different approaches are needed to determine solute partitioning into the liquid (interfacial brine) and solid (ice matrix) phases for the two scenarios described above. We discuss the two approaches below. The notations used in the following discussion differ slightly from those used in Eqs. (1–5) and (7) and are based on a generic gas phase molecule HA, which dissociates completely in the brine to form H^+ and A^-.

2.3.1 Known melt solute concentration

If the solute mole fraction in a melted snow/ice sample is known, we have the model input $x_{\mathrm{I},0} = x_{\mathrm{H},0} + x_{\mathrm{A},0}$, which is the total solute-ion mole fraction in the melted sample. Note that here the notation $x_{\mathrm{I},0}$ is used instead of $x_{\mathrm{HA},0}$ in order to highlight the fact that molecular HA dissociates in aqueous media, and the solute mole fraction in the solution is the sum of the mole fractions of the ions present. Likewise, x_{I}, the total solute mole fraction in the brine layer, is equal to $(x_{\mathrm{H}} + x_{\mathrm{A}})$. Since our model molecule HA is assumed to dissociate completely, $x_{\mathrm{H}} = x_{\mathrm{A}}$ in this case. Solving Eq. (1), we obtain x_{I}. Assuming brine-gas equilibrium, the partial pressure of the solute in the gas phase can be predicted by Henry's law (Eq. 6), and the partitioning of solute to the ice matrix can be determined using Eq. (7). We can then find the brine mole fraction, φ, for which mass balance closure is achieved:

$$x_{\mathrm{I},0}=x_{\mathrm{I}}\varphi+x_{\mathrm{HA}}^{\mathrm{ice}}(1-\varphi) \tag{8}$$

From here on Eqs. (4) and (5) can be used to calculate the brine volume fraction and thickness.

2.3.2 Known partial pressure

In the scenario in which the partial pressure of the acid is known but solute content of the condensed phase is unknown, Eq. (7) can be used to calculate the mole fraction of acid in ice ($x_{\mathrm{HA}}^{\mathrm{ice}}$) at equilibrium. Equation (6) can be used to solve for x_{A} , but since γ_{A} is itself a function of x_{A}, an iterative solution is required. In order to calculate the brine mole fraction, another iterative loop is triggered, in which the brine mole fraction, φ, is varied until the x_{A} calculated using Eq. (1) matches that obtained by Henry's law. Using the converged φ, Eqs. (4) and (5) can be applied to obtain φ_V and d_{BL}.

In Sect. 3.2, we show examples demonstrating the application of the model to the HNO_3-H_2O and HCl-H_2O systems.

3 Results and discussion

In the following paragraphs, we apply the model to several different scenarios and demonstrate its ability to predict relevant quantities, such as brine volume fraction, thicknesss and brine composition.

3.1 Application to the NaCl-H_2O sytem

Surface brine layers on sea ice are known to be chemically important, and many studies have been done to probe the freeze concentration effect (Cheng et al., 2009; Conklin and Bales, 1993; Foster et al., 2001; Michalowski et al., 2000; Cho et al., 2002). Cho et al. (2002) derived a thermodynamic model to predict the fraction of liquid water in the surface brine layer formed upon freezing of a salt-containing solution, assuming low solute concentration and ideal solution behavior. In real environmental systems, however, brine layers are likely to be highly concentrated and therefore exhibit deviations from ideality. Akinfiev et al. (2001) used experimental data for the NaCl-H_2O system to derive a set of Pitzer equation parameters, which can be used to calculate the ionic activity coefficient $\gamma_{\pm}$ of NaCl in an aqueous solution at subzero temperatures.

Using the computing software MATLAB® (R2011a, MathWorks), we created an algorithm which incorporates the Pitzer parameterizations given by Akinfiev et al. (2001), to solve Eq. (1) numerically for the concentration of NaCl in the brine, evaluate the non-ideality index, and estimate the volume fraction of the brine for a range of temperatures at a given melt concentration, $x_{\mathrm{s},0}$, specified by the user.

Figure 1 shows the results for brine volume fraction and the non-ideality index for a range of NaCl concentrations. Note that the NaCl concentrations in the legend of Fig. 1 are those of the completely melted sample. The highest concentration (1.12 m) approximates the salt content of sea water. Figure 1a shows that brine volume fraction increases rapidly with the amount of salt present in the system. For a given initial concentration, φ_V decreases gradually as temperature drops from T_{m} and then remains fairly constant as it approaches the eutectic temperature, which is marked by the dotted vertical line in Fig. 1. From Fig. 1b, one can see that the effect of non-ideality can become significant, especially at low temperatures and for systems with higher salt content.

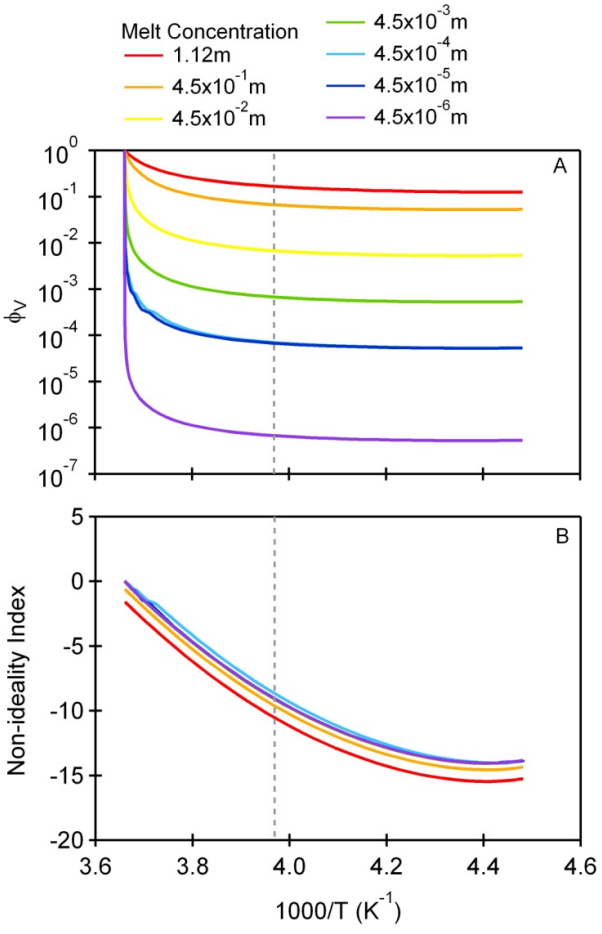

Fig. 1. Calculated **(A)** brine volume fraction and **(B)** the non ideality index of the brine layer at different NaCl concentrations in the melt and at a range of temperatures.

Cho et al. (2002) used NMR to determine the salt concentration in the brine layer formed upon freezing of sea water and compared the experimental results to a thermodynamic model derived assuming low solute concentration (similar to Eq. 2). Figure 2 shows the volume fraction predicted by both models as well as Cho et al.'s NMR data for sea water. At lower temperatures, our model can more accurately reproduce the experimental data by capturing the effect of non-ideality. Although good agreement exists between our model and the experimental data of Cho et al. at sub-eutectic temperatures, one should use caution in interpreting the results from the model in this temperature range since it does not take into account solid formation.

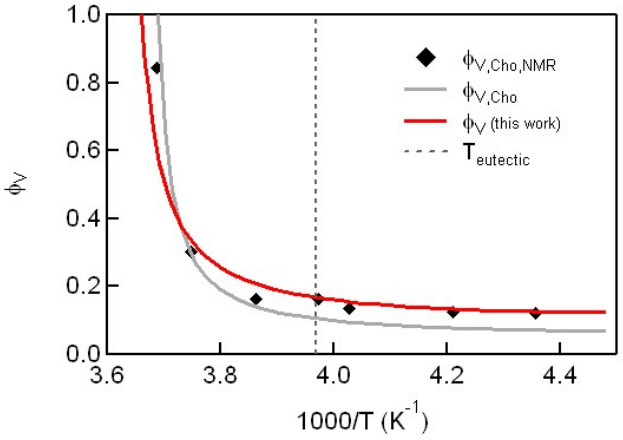

Fig. 2. Volume fraction of brine layer on frozen sea water extracted from NMR data by Cho et al. (2002) as a function of temperature. The solid gray line represents the calculated volume fraction of the brine layer using Cho's model. The solid red line represents the calculated thickness of the brine layer using the BL model in this study. The eutectic temperature is marked by the dotted vertical line.

3.2 Application to soluble gas-phase acids

In this section we demonstrate the application of the model to the HNO_3-H_2O system and the HCl-H_2O system. In both cases, three scenarios will be discussed: (1) the total solute content in the condensed phase is known, (a) with or (b) without additional solute partitioning to the gas phase and ice matrix, and (2) known gas-phase composition but unknown condensed phase composition. HNO_3 and HCl are of course volatile solutes that are known to diffuse into the ice matrix to a limited extent, but application of scenario (1b) allows us to compare our model to existing models which neglect solute partitioning among the three phases. We then apply the model to conditions representative of laboratory studies of trace gas-ice interactions.

3.2.1 HNO_3-H_2O system

Nitric acid is known to have active roles in the heterogeneous chemistry of polar stratospheric clouds (PSC) and stratospheric ozone destruction (Tisdale et al., 1999; Tolbert and Middlebrook, 1990). In the presence of water, nitric acid can dissociate to form nitrate ions. Nitrate is photo-active in the actinic region. The photolysis of nitrate ions in liquid layers on ice is believed to play a role in HONO and NOx production in snow (Boxe et al., 2005; Boxe and Saiz-Lopez, 2008; Honrath et al., 1999; Mack and Bolton, 1999). Figure 3 shows the application of the model to the HNO_3-ice system assuming the first scenario (non-volatile solute, no equilibration with the gas phase or incorporation into the ice matrix). Non-ideal solution behavior is taken into account as described by Eq. (1). In this graph, the brine volume

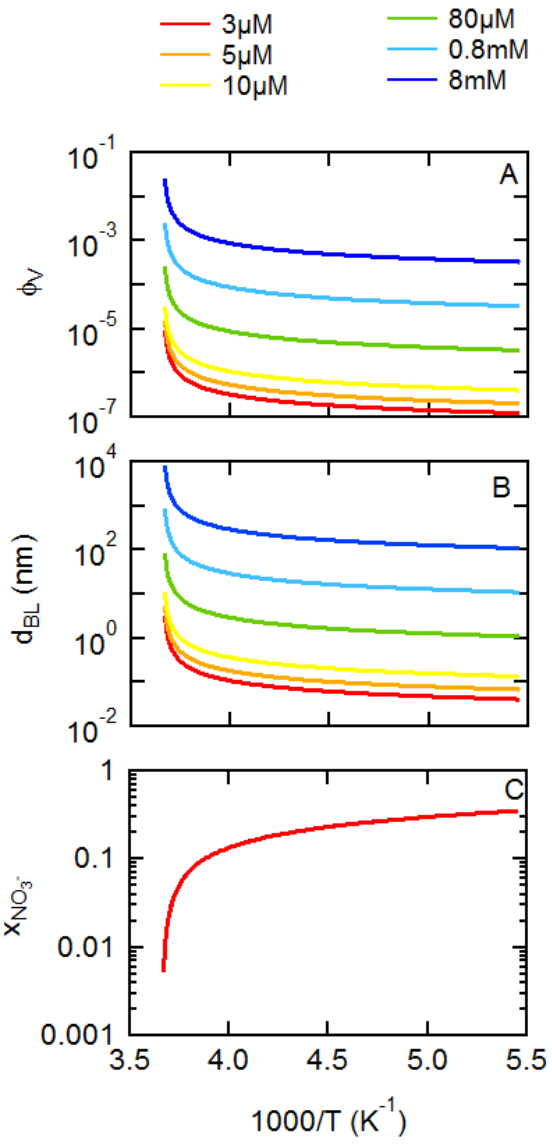

Fig. 3. Model prediction based on non-volatile solute scenario of **(A)** brine volume fraction, **(B)** brine thickness calculated assuming spherical ice crystals, 1 mm in radius, and **(C)** nitrate mole fraction in the brine at different nitrate concentrations in the melt and at a range of temperatures using the full model which accounts for non-ideal behavior.

fraction (Fig. 3a), the brine layer thickness (Fig. 3b) and the brine mole fraction of NO_3^- (Fig. 3c) are plotted as a function of inverse temperature and at different concentrations (the concentrations in the legend represent the total concentration in the melt). Note that brine layer thickness was calculated for Figs. 3–6 assuming spherical ice crystals, 1 mm in radius (Thomas et al., 2011). The chosen concentrations ranged from 3 μM (coastal Antarctic snowpack) (Boxe and Saiz-Lopez, 2008) to 8 mM (similar to cirrus ice composition observed by Voigt et al., 2007). As the concentration of

HNO_3 increases, the brine layer thickness and volume fraction also increase, reaching a maximum at the melting temperature of ice. At a given melt concentration, the thickness of the BL decreases with decreasing temperatures, while solute mole fraction increases (Fig. 3c), illustrating the process of freeze concentration. As shown in Fig. 3c, the mole fraction profiles for the various melt concentrations 3 µM–8 mM overlap. This phenomenon can be understood by recalling Eq. (2) (which is a simplified form of Eq. 1), in which $x_{s,0}$ appears only in the term $(1-x_{s,0})$, which is approximately equal to 1 for small $x_{s,0}$. As the brine becomes more concentrated, its solution behavior is expected to become less ideal. We re-ran the model assuming ideal solution behavior by using Eq. (2) to solve for x_I. Plots for the ideal case are shown in Fig. S1 in the Supplement. Curves for a melt concentration of 10 µM are shown together along with the Cho et al. (2002) model in Fig. 4. We find that the ideal solution assumption as applied in this model and by Cho and coworkers results in an underestimation of the brine volume fraction and thickness and an overestimation of the nitrate mole fraction in the brine. At a melt concentration of 10 µM, the ideal solution assumption leads to an underestimate of the volume fraction by more than 30 % at temperatures below 246 K.

Figure 5 shows the effect of enforcing equilibration of HNO_3 in the brine with the gas phase and the ice matrix on the brine volume fraction (Fig. 5a), thickness (Fig. 5b) and the nitrate mole fraction in the brine (Fig. 5c). When comparing Fig. 3 to Fig. 5, one sees that when solute partitioning to the ice matrix is taken into account, predictions of φ_V and d_{BL} are lower at low temperatures, due to the increased solubility in the ice matrix (see Eq. 8). If we take the same system but now assume that the brine is an ideal solution by setting the non-ideality index term in Eq. (1) to zero (see Fig. S2, in the Supplement), it again predicts lower φ_V and d_{BL} than the non-ideal case. Predictions for brine volume fraction, layer thickness, and brine composition are shown using the gas-brine-ice equilibrium model for a total melt concentration of 10 µM NO_3^- for comparison with the other models in Fig. 4. Note that for a given fixed melt composition, the prediction of brine composition is determined not by model but by whether or not the ideal solution assumption was used.

Note that using the gas-brine-ice equilibrium model for a given fixed total solute content typical of melted snow samples can lead to relatively high predicted gas phase concentration. For example, at a melt concentration of 3 µM and at 245 K, the predicted gas phase HNO_3 concentration was 194 ppb. The concentration is 1000 times more than gas phase concentration observed at snow surface in Summit, Greenland (Thomas et al., 2011). Gas-phase concentrations of species which are generated in the snowpack may be elevated $> 10\times$ in firn air as compared to the ambient air (Thomas et al., 2011). However, it is also likely that some of the brine in the snow sample was not in contact with air prior to melting (i.e. was present in a grain boundary, triple junction or micropocket), or that equilibrium is not reached for volatile species generated in the snowpack, and for these reasons Henry's law equilibrium between the gas and brine may not be fully manifested.

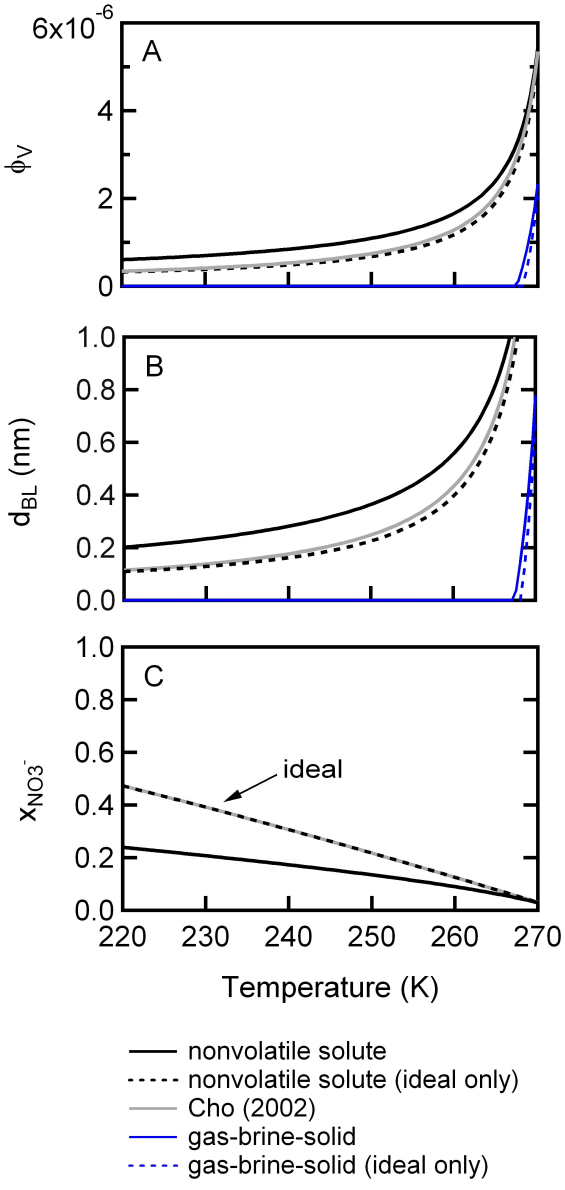

Fig. 4. Model comparison for a melt concentration of 10 µM HNO_3. **(A)** Brine volume fraction, **(B)** brine thickness calculated assuming spherical ice crystals, 1mm in radius and **(C)** nitrate mole fraction in the brine are shown using our models assuming nonvolatile solute (black) or enforcing solute partitioning among the gas, brine, and ice matrix (blue). Results from the full models which account for non-ideal behavior (solid lines) or assuming ideal behavior (dashed lines) are shown. Predictions from the model of Cho et al. (2002) are shown for comparison (grey line).

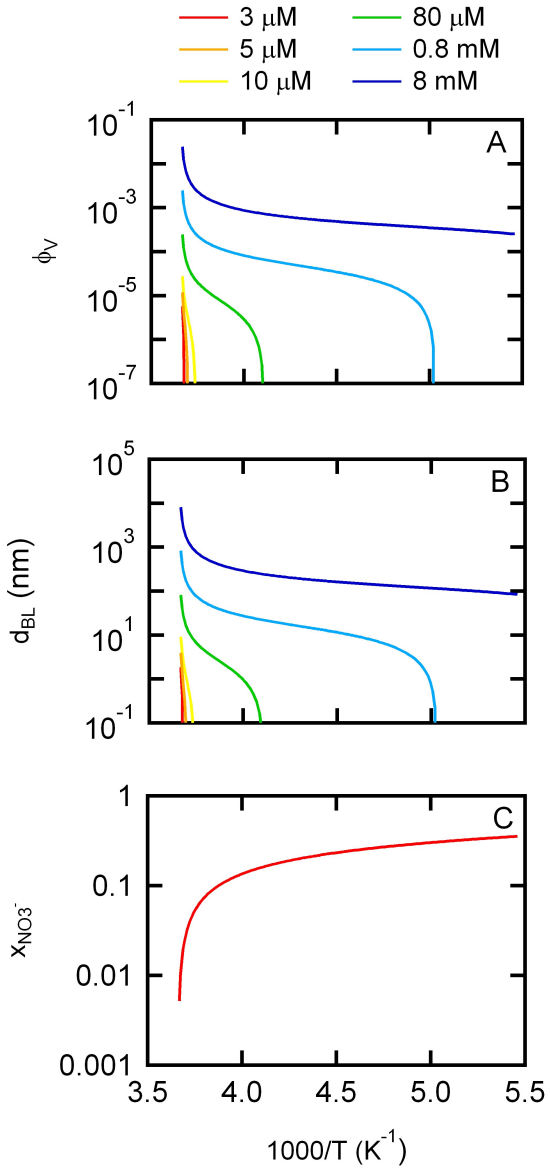

Fig. 5. Model prediction for the scenario where solute partitioning is allowed based on gas-brine and gas-ice equilibrium for **(A)** brine volume fraction, **(B)** brine thickness calculated assuming spherical ice crystals, 1 mm in radius and **(C)** nitrate mole fraction in the brine at different nitrate concentrations in the melt and a range of temperatures using the full model which accounts for non-ideal behavior.

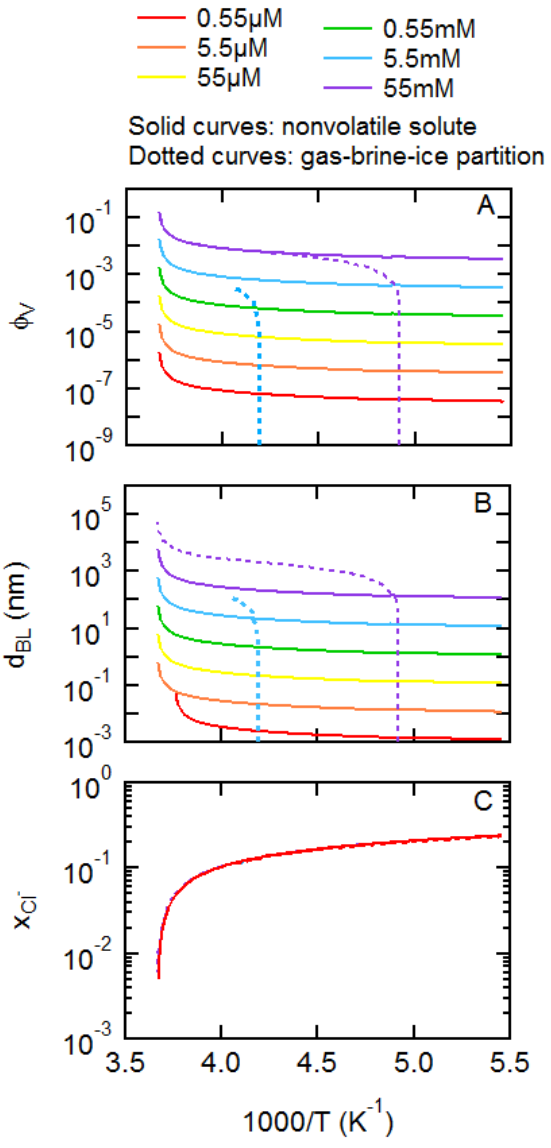

Fig. 6. Model prediction of **(A)** brine volume fraction, **(B)** brine thickness calculated assuming spherical ice crystals, 1mm in radius and **(C)** chloride mole fraction in the brine at different chloride concentrations in the melt and at a range of temperatures using the full model which accounts for non-ideal behavior. The solid lines represent the non-volatile solute scenario. The dotted lines represent a partitioning scenario based on gas-brine and gas-ice equilibrium.

3.2.2 HCl-H_2O system

HCl has been shown to play a catalytic role in the destruction of stratospheric ozone (Molina et al., 1987). In aqueous systems, HCl can dissociate to form chloride ions. In the polar boundary layer, chloride is highly active and can be oxidized to form reactive halogen species in air that can lead to the depletion of ozone in the boundary layer (Simpson et al., 2007). Similar to the analysis we presented in the previous section for HNO_3, for the situation in which the melt solute concentration is known, we apply our model to calculate the mole fraction of chloride ions in the brine using two different methods: (1) assuming that the dissolved acid is non-volatile and does not partition to the gas phase or the ice matrix, and (2) enforcing equilibrium partitioning of HCl among the gas, brine, and ice phases. For each of the two methods, we run the model using either Eq. (1) or Eq. (2) to calculate the chloride mole fraction in the brine to investigate the effect

of accounting for non-ideal solution behavior. Figure S3 (in the Supplement) shows the results obtained when the system is assumed to be ideal (i.e. calculate x_{Cl^-} using Eq. 2), and Fig. 6 shows the results obtained when non-ideality is considered (Eq. 1). Solid curves in Figs. S3 and 6 represent cases where the chloride is assumed to be non-volatile, whereas dotted curves are for cases where brine-gas and gas-ice equilibrium conditions are enforced. The concentrations in the legend are those of the completely melted sample and encompass the range encountered in the natural environment. The primary observation in both Figs. 6 and S3 is the major difference in the shape of the φ_V and d_{BL} curves when different assumptions about solute partitioning are used. Whereas φ_V and d_{BL} persist down to very low temperatures when the solute is treated as non-volatile, both quantities show a drop-off to zero as the temperature decreases when partitioning is allowed. In addition, when the solute is treated as non-volatile, different melt concentrations yielded distinct curves for φ_V and d_{BL}. However, when the solute is allowed to partition to the gas and ice matrix, as we observed for the HNO_3-ice system, the mole fraction of chloride ion in the brine did not depend significantly on melt concentration.

When comparing Fig. 6 (non-ideal) and Fig. S3 (ideal), one sees that, consistent with the results for HNO_3, the ideal model consistently under-predicts φ_V and d_{BL} and over-predicts x_{Cl^-}. Another key observation is that when the ideal model is used (Fig. S3), and we allow solute partitioning to the gas and ice matrix (dotted curves), φ_V and d_{BL} vanish at much higher temperatures than that observed when non-ideality is taken into account (Fig. 6 dotted curves).

Generally, Figs. 6 and S3 clearly illustrate that the brine volume fraction and thickness predicted by the model can differ greatly when different assumptions are used. Thus, the user must carefully analyze which set of assumptions are best suited for the system being studied. The above examples demonstrate the use of the model when the solute mole fraction in the melt is known. In controlled laboratory environments, it is more likely that one may wish to apply this model to predict the volume fraction or thickness of an interfacial layer, knowing the partial pressure of the gaseous acid to which the ice is exposed. An example is provided in the following section for such a situation.

3.2.3 Application to laboratory studies of trace gas-ice interactions

Laboratory studies investigating trace gas-ice interactions often make use of ice samples with very low initial impurity concentrations. The model presented here can be used as a valuable tool to identify the presence of brine and characterize the properties of any existing brine layer under conditions relevant to laboratory experiments. Applying our model to conditions similar to the NEXAFS study of HNO_3 uptake to ice by Krepelova et al. (2010) (7.5×10^{-7} torr and at 231 K) we predict no brine layer formation, consistent with their experimental finding that neither BL nor QLL was present.

Using the method described in the Sect. 3.3.2, we calculated brine volume fraction and thickness for four HCl partial pressures spanning the HCl-ice regime on the HCl-H_2O phase diagram (McNeill et al., 2006) which have recently been examined for interfacial layer formation using ellipsometry (McNeill et al., 2006, 2007). For all four partial pressures tested (1×10^{-7}, 5×10^{-7}, 2×10^{-6}, and 1×10^{-5} torr HCl), no appreciable layer formation was found until the temperature is raised to a few degrees K below the bulk melting point. McNeill et al. (2006, 2007) detected a disordered surface layer using ellipsometry (at 2×10^{-6} torr HCl at 218 K). They calculated the solubility of HCl into this layer and found that it was intermediate between that of a true liquid and that of ice – i.e. a "quasi-liquid". They also demonstrated that the presence of the layer greatly influenced the $ClONO_2$ + HCl surface reaction and HCl-CH_3COOH coadsorption. We tested the conditions used in the experiments by McNeill et al. (2006, 2007) using our model and determined that a true liquid layer (i.e. brine layer) is not present, consistent with their interpretation that the layer they observed was a quasi-liquid, rather than a true interfacial solution.

4 Summary and outlook

We have developed a model for liquid brine layers on environmental ice systems that is valid across a wide compositional range and for temperatures relevant to the Polar Regions and the upper atmosphere. In the environment, the composition and properties of the air-ice interface are constantly changing. Our model, because it can be applied over a wide range of temperatures and compositions and enforces equilibration among the brine, the gas, and the ice matrix, can be used to describe this dynamically evolving interface. The modeling method is highly versatile and can be easily adapted to a variety of systems. In the examples used herein, we applied the model to single-solute systems. However, systems containing multiple solutes can be treated using the same general framework by incorporating appropriate expressions for activity coefficients which take into account solute-solute interactions (Chan et al., 1997; Clegg et al., 1998a, b, 2001; Clegg and Seinfeld, 2006a, b; Clegg and Simonson, 2001; Massucci et al., 1999; Rard et al., 2003, 2010; Tong et al., 2008; Wexler and Clegg, 2002). This model can be also applied to organic solutes granted that the Henry's law constant, activity, and solubility for these species in ice are known as a function of temperature (Clegg et al., 2001; Clegg and Seinfeld, 2006a, b; Tong et al., 2008; Barret et al., 2010).

The parameters used here to calculate the interfacial layer thickness in each test case were based on experimental data from the literature. However, many of the physical

Table 1. Conditions for which the brine volume fraction, φ_V, is less than 3×10^{-5} as predicted by the model under various scenarios. This cutoff value of φ_V corresponds to a brine layer of 10 nm on a sphere with radius 1 mm.

NaCl (Non-volatile solute)	
$NaCl-H_2O$:	$\phi_V > 3\times10^{-5}$ for [$223 < T < 273$ K]* and $m_{NaCl,0} > 5\times10^{-9}$ mol kg^{-1}
HNO_3 and HCl	
Scenario 1a: known solute content in melt, no partitioning to ice and gas phases	
HNO_3-H_2O:	$\phi_V < 3\times10^{-5}$ for $C_{NO_3,0} < 80$ µM and at $T <$ 269 and $\phi_V < 3\times10^{-5}$ for $C_{NO_3,0} < 10$ µM in the range [$180 < T < 273$ K]
$HCl-H_2O$:	$\phi_V < 3\times10^{-5}$ for $C_{Cl,0} < 55$ µM and at $T <$ 269 K $\phi_V < 3\times10^{-5}$ for $C_{Cl,0} < 5.5$µM in the range [$180 < T < 273$ K]
Scenario 1b: known solute content in melt, with gas-brine-ice equilibrium	
HNO_3-H_2O:	$\phi_V < 3\times10^{-5}$ for [$180 < T < 273$ K] and [3 µM $< C_{NO_3,0} < 10$ µM] and $\phi_V < 3\times10^{-5}$ for $T < 268$ K and $C_{NO_3,0} \leq 80$ µM and $\phi_V < 3\times10^{-5}$ for $T < 218$ and $C_{NO_3,0} \leq 800$ µM
$HCl-H_2O$:	$\phi_V < 3\times10^{-5}$ for $C_{Cl,0} < 5.5$ mM and at $T <$ 239 K
Scenario 2: known gas phase composition, unknown condensed phase composition	
HNO_3-H_2O:	$\phi_V < 3\times10^{-5}$ for $T < 269$ K in the range [$9\times10^{-9} < p_{HNO_3} < 1\times10^{-5}$ torr] or $p_{HNO_3} < 1\times10^{-7}$ torr in the range [$200 < T < 273$ K]
$HCl-H_2O$:	$\phi_V < 3\times10^{-5}$ for $T <$ 266K in the range [$1\times10^{-8} < p_{HCl} < 5\times10^{-5}$ torr] or $p_{HCl} < 2\times10^{-7}$ torr in the range [$200 < T <$ 273 K]

* Note that the eutectic temperature of this system is 252.05 K (−21.1 °C).

parameters of ice in complex environmental systems have yet to be quantified experimentally. For example, the solubility of key trace gases in ice will need to be measured in order to accurately model not just the chemistry of the air-ice interface, but the thickness of the liquid layer. More laboratory studies of interfacial layer thickness as a function of temperature and impurity load for different solutes are needed for model validation. Particularly, the effect of organic material on liquid layer thickness and composition has not yet been investigated. Finally, complete and precise knowledge of the level of impurities in environmental systems, a key variable for determining the thickness of the liquid layers at the air-ice interface, is often not available. This underscores the importance of measurements of snow/ice composition, morphology and air composition for understanding air-ice chemical interactions in Polar Regions.

The HCl-ice example in Sect. 3.2.2 highlights an important fact that modelers interested in the effect of interfacial layers on chemistry, for example, should always bear in mind: under relatively pristine conditions for which the a brine layer is not predicted, a quasi-liquid layer may still be present and can significantly affect interfacial chemistry. Table 1 summarizes scenarios for which our model predicted very little or no brine formation (we assign a cutoff of $\varphi_V \leq 3 \times 10^{-5}$, which corresponds to a brine layer of 10 nm on a sphere with radius 1 mm). A model such as that of Wettlaufer (1999) may be used to predict the QLL thickness at very low impurity concentrations. However, we stress

caution when modeling interfacial chemistry based on such a calculation, since at this time very little is known about the relationship between the extent of the QLL and interfacial chemistry.

Appendix A

List of symbols and their definitions

Symbol	Quantity
T	System temperature
T_m	Bulk melting temperature of pure ice (273.15 K)
P	System pressure
ΔH_w^{fus}	Enthalpy of fusion of water
R	Gas constant
x_s	Mole fraction of solute in brine
$x_{s,0}$	Mole fraction of solute in unfrozen solution
x_I	Sum of all solute-ion mole fractions in brine
$x_{I,0}$	Sum of all solute-ion mole fractions in unfrozen solution
x_s^{ice}	Mole fraction of solute in ice matrix
$x_{H,0}$	Mole fraction of ion H^+ in unfrozen solution
$x_{A,0}$	Mole fraction of ion A^- in unfrozen solution
x_{HA}^{ice}	Mole fraction of HA in ice matrix
γ_s	Activity coefficient of solute in brine
γ_H	Activity coefficient of ion H^+ in brine
γ_A	Activity coefficient of ion A^- in brine
$\gamma_\pm$	Mean ionic activity coefficient
K_H	Henry's law constant
p_s	Partial pressure of solute in gas phase
p_{HA}	Partial pressure of molecule HA in gas phase
A_0	Proportionality constant in equation 7
Δh_s^{sub}	Partial molar enthalpy of sublimation of s from ice
n	Ice vapor pressure depression factor in equation 7
φ	Mole fraction of molecules in brine (water + solutes)
φ_V	Volume fraction of brine
M_{brine}	Mole-fraction-weighted molar mass of brine
M_{total}	Mole-fraction-weighted molar mass of entire sample
n_w^{brine}	Moles of water in brine layer
n_s^{brine}	Moles of solute in brine layer
n_w	Total number of moles of water in sample
n_s	Total number of moles of solute in sample
d_{BL}	Thickness of liquid layer
V	Volume of ice sample
A	Surface area of ice sample
ρ_{brine}	Density of brine
ρ_{total}	Density of entire ice sample

Supplementary material related to this article is available online at: http://www.atmos-chem-phys.net/11/9971/2011/acp-11-9971-2011-supplement.pdf.

Acknowledgements. This work was funded by a NSF CAREER award for VFM (ATM-0845043). The authors would like to thank Sanat Kumar for helpful discussions and suggestions during the development of the mathematical model presented in this work.

Edited by: M. Petters

References

Akinfiev, N. N., Mironenko, M. V., and Grant, S. A.: Thermodynamic Properties of NaCl Solutions at Subzero Temperatures, J. Solution Chem., 30, 1065–1080, 2001.

Anisimov, O. A., Vaughan, D. G., Callaghan, T. V., Furgal, C., Marchant, H., Prowse, T. D., Vilhjalmsson, H., and Walksh, J. E.: Polar regions (Arctic and Antarctic), in Climate Change 2007: Impacts, Adaptation, and Vulnerability, Contribution of Working Group II to the Fourth Assessment Report of the Intergovernmental Panel on Climate Change, edited by: Parry, M. L., Canziani, O. F., Palutikof, J. P., van der Linden, P. J., and Hanson, C. E., 653–685, Cambridge University Press, Cambridge, 2007.

Baker, I., Cullen, D., and Iliescu, D.: The microstructural location of impurities in ice, Can. J. Phys., 81, 1–9, 2003.

Baker, I., Obbard, R., Iliescu, D., and Meese, D.: Microstructural characterization of firn, Hydrol. Process., 21, 1624–1629, 2007.

Barret, M., Houdier, S., and Domine, F.: Thermodynamics of the FormaldehydeWater and FormaldehydeIce Systems for Atmospheric Applications, J. Phys. Chem. A, 115, 307–317, 2010.

Bartels-Rausch, T., Guimbaud, C., Gaggeler, H. W., and Ammann, M.: The partitioning of acetone to different types of ice and snow between 198 and 223 K, Geophys. Res. Lett., 31, L16110, doi:10.1029/2004GL020070, 2004.

Boxe, C. S. and Saiz-Lopez, A.: Multiphase modeling of nitrate photochemistry in the quasi-liquid layer (QLL): implications for NO_X release from the Arctic and coastal Antarctic snowpack, Atmos. Chem. Phys., 8, 4855–4864, doi:10.5194/acp-8-4855-2008, 2008.

Boxe, C. S., Colussi, A. J., Hoffmann, M. R., Murphy, J. G., Wooldridge, P. J., Bertram, T. H., and Cohen, R. C.: Photochemical production and release of gaseous NO_2 from nitrate-doped water ice, J. Phys. Chem. A, 109, 8520–8525, 2005.

Carslaw, K. S., Clegg, S. L., and Brimblecombe, P.: A Thermodynamic Model of the System Hcl-HNO_3-H_2SO_4-H_2O, Including Solubilities of HBr, from <200 to 328 K, J. Phys. Chem., 99, 11557–11574, 1995.

Chan, C. K., Liang, Z., Zheng, J. A., Clegg, S. L., and Brimblecombe, P.: Thermodynamic properties of aqueous aerosols to high supersaturation: I- Measurements of water activity of the system Na^+-Cl-NO_3-SO_4^{2-}-H_2O at ∼298.15 K, Aerosol Sci. Technol., 27, 324–344, 1997.

Cheng, J., Soetjipto, C., Hoffmann, M. R., and Colussi, A. J.: Confocal Fluorescence Microscopy of the Morphology and Composition of Interstitial Fluids in Freezing Electrolyte Solutions, J. Phys. Chem. Lett., 1, 374–378, 2009.

Cho, H., Shepson, P. B., Barrie, L. A., Cowin, J. P., and Zaveri, R.: NMR investigation of the quasi-brine layer in ice/brine mixtures, J. Phys. Chem. B, 106, 11226–11232, 2002.

Clegg, S. L. and Brimblecombe, P.: Equilibrium Partial Pressures and Mean Activity and Osmotic Coefficients of 0–100 % Nitric-Acid as a Function of Temperature, J. Phys. Chem., 94, 5369–5380, 1990.

Clegg, S. L. and Seinfeld, J. H.: Thermodynamic models of aqueous solutions containing inorganic electrolytes and dicarboxylic acids at 298.15 K. 2. Systems including dissociation equilibria, J. Phys. Chem. A, 110, 5718–5734, 2006a.

Clegg, S. L. and Seinfeld, J. H.: Thermodynamic models of aqueous solutions containing inorganic electrolytes and dicarboxylic

acids at 298.15 K. 1. The acids as nondissociating components, J. Phys. Chem. A, 110, 5692–5717, 2006b.

Clegg, S. L. and Simonson, J. M.: A BET model of the thermodynamics of aqueous multicomponent solutions at extreme concentration, J. Chem. Thermo. , 33, 1457–1472, 2001.

Clegg, S. L. and Wexler, A. S.: Densities and Apparent Molar Volumes of Atmospherically Important Electrolyte Solutions. 1. The Solutes H_2SO_4, HNO_3, HCl, Na_2SO=, $NaNO_3$, NaCl, $(NH_4)_2SO_4$, NH_4NO_3, and NH_4Cl from 0 to 50 °C, Including Extrapolations to Very Low Temperature and to the Pure Liquid State, and $NaHSO_4$, NaOH, and NH_3 at 25 °C, J. Phys. Chem. A, 115, 3393–3460, 2011.

Clegg, S. L., Brimblecombe, P., and Wexler, A. S.: Thermodynamic model of the system H^+-NH_4^+-Na^+-SO_4^{2-}-NO_3-Cl-H_2O at 298.15 K, J. Phys. Chem. A, 102, 2155–2171, 1998a.

Clegg, S. L., Brimblecombe, P., and Wexler, A. S.: Thermodynamic model of the system H^+-NH_4^+-Na^+-SO_4^{2-}-NO_3-H_2O at tropospheric temperatures, J. Phys. Chem. A, 102 , 2137–2154, 1998b.

Clegg, S. L., Seinfeld, J. H., and Brimblecombe, P.: Thermodynamic modelling of aqueous aerosols containing electrolytes and dissolved organic compounds, J. Aerosol Sci., 32, 713–738, 2001.

Conklin, M. H. and Bales, R. C.: SO_2 Uptake on Ice Spheres: Liquid Nature of the Ice-Air Interface, J. Geophys. Res.-Atmos., 98, 16851–16855, 1993.

Cullen, D. and Baker, I.: The chemistry of grain boundaries in Greenland ice, J. Glaciol., 46, 703–706, 2000.

Denman, K. L., Brasseur, G., Chidthaisong, A., Ciais, P., Cox, P. M., Dickenson, R. E., Hauglustaine, D., Heinze, C., Holland, E., Jacob, D. J., Lohmann, U., Ramachandran, S., da Silva Dias, P. L., Wofsy, S. C., and Zhang, X.: Couplings Between Changes in the Climate System and Biogeochemistry, in: Climate Change 2007: The Physical Science Basis. Contribution of Workign Group I to the Fourth Assessment Report of the Intergovernmental Panel on Climate Change, edited by: Solomon, S., Qin, D., Manning, M., Chen, Z., Marquis, M., Averyt, K. B., Tignor, M., and Miller, H. L., Cambridge University Press, Cambridge, 2007.

Domine, F. and Shepson, P. B.: Air-Snow Interactions and Atmospheric Chemistry, Science, 297, 1506–1510, 2002.

Foster, K. L., Plastridge, R. A., Bottenheim, J. W., Shepson, P. B., Finlayson-Pitts, B. J., and Spicer, C. W.: The Role of Br_2 and BrCl in Surface Ozone Destruction at Polar Sunrise, Science, 291, 471–474, 2001.

Fukazawa, H., Sugiyama, K., Mae, S. J., Narita, H., and Hondoh, T.: Acid ions at triple junction of Antarctic ice observed by Raman scattering, Geophys. Res. Lett., 25, 2845–2848, 1998.

Gamblin, B., Toon, O. B., Tolbert, M. A., Kondo, Y., Takegawa, N., Irie, H., Koike, M., Ballenthin, J. O., Hunton, D. E., Miller, T. M., Viggiano, A. A., Anderson, B. E., Avery, M., Sachse, G. W., Podolske, J. R., Guenther, K., Sorenson, C., and Mahoney, M. J.: Nitric acid condensation on ice: 1. Non-HNO_3 constituent of NO_Y condensing upper tropospheric cirrus particles, J. Geophys. Res.-Atmos., 111, D21203, doi:10.1029/2005JD006048, 2006.

Gamblin, B., Toon, O. B., Tolbert, M. A., Kondo, Y., Takegawa, N., Irie, H., Koike, M., Hudson, P. K., Ballenthin, J. O., Hunton, D. E., Miller, T. M., Viggiano, A. A., Anderson, B. E., Avery, M., Sachse, G. W., Guenther, K., Sorenson, C., and Mahoney, M. J.: Nitric acid condensation on ice: 2. Kinetic limitations, a possible "cloud clock" for determining cloud parcel lifetime, J. Geophys. Res.-Atmos., 112, D12209, doi:10.1029/2005JD006049, 2007.

Gao, R. S., Popp, P. J., Fahey, D. W., Marcy, T. P., Herman, R. L., Weinstock, E. M., Baumgardner, D. G., Garrett, T. J., Rosenlof, K. H., Thompson, T. L., Bui, P. T., Ridley, B. A., Wofsy, S. C., Toon, O. B., Tolbert, M. A., Karcher, B., Peter, T., Hudson, P. K., Weinheimer, A. J., and Heymsfield, A. J.: Evidence that nitric acid increases relative humidity in low-temperature cirrus clouds, Science, 303, 516–520, 2004.

Grannas, A. M., Jones, A. E., Dibb, J., Ammann, M., Anastasio, C., Beine, H. J., Bergin, M., Bottenheim, J., Boxe, C. S., Carver, G., Chen, G., Crawford, J. H., Dominé, F., Frey, M. M., Guzmán, M. I., Heard, D. E., Helmig, D., Hoffmann, M. R., Honrath, R. E., Huey, L. G., Hutterli, M., Jacobi, H. W., Klán, P., Lefer, B., McConnell, J., Plane, J., Sander, R., Savarino, J., Shepson, P. B., Simpson, W. R., Sodeau, J. R., von Glasow, R., Weller, R., Wolff, E. W., and Zhu, T.: An overview of snow photochemistry: evidence, mechanisms and impacts, Atmos. Chem. Phys., 7, 4329–4373, doi:10.5194/acp-7-4329-2007, 2007a.

Grannas, A. M., Bausch, A. R., and Mahanna, K. M.: Enhanced aqueous photochemical reaction rates after freezing, J. Phys. Chem. A, 111, 11043–11049, 2007b.

Harrison, W. D. and Raymond, C. F.: Impurities and Their Distribution in Temperate Glacier Ice, J. Glaciol., 16, 173–181, 1976.

Honrath R. E., Peterson M. C., Guo, S., Dibb, J. E., Shepson, P. B., and Cambell, B.: Evidence of NO_x production within or upon ice particles in the Greenland snowpack, Geophys. Res. Lett., 26, 695–698, 1999.

Huthwelker, T., Lamb, D., Baker, M., Swanson, B., and Peter, T.: Uptake of SO_2 by Polycrystalline Water Ice, J. Colloid Interf. Sci., 238, 147–159, 2001.

Krepelova, A., Newberg, J., Huthwelker, T., Bluhm, H., and Ammann, M.: The nature of nitrate at the ice surface studied by XPS and NEXAFS, Phys. Chem. Chem. Phys., 12, 8870–8880, 2010.

Lemke, P., Ren, J., Alley, R. B., Allison, I., Carrasco, J., Flato, G., Fujii, Y., Kaser, G., Mote, P., Thonas, R. H., and Zhang, T.: Observations: Changes in Snow, Ice, and Frozen Ground, in: Climate Change 2007: The Physical Science Basis. Contribution of Working Group I to the Fourth Assessment Report of the Intergovernmental Panel on Climate Change, edited by: Solomon, S., Qin, D., Manning, M., Chen, Z., Marquis, M., Averyt, K. B., Tignor, M., and Miller, H. L., Cambridge, United Kingdom and New York, NY, USA, Cambridge University Press, Ref Type: Report, 2007.

Liao, W. and Tan, D.: 1-D Air-snowpack modeling of atmospheric nitrous acid at South Pole during ANTCI 2003, Atmos. Chem. Phys., 8, 7087–7099, doi:10.5194/acp-8-7087-2008, 2008.

Maccagnan, M. and Duval, P.: Electric behavior of Antarctic ice and radio echo layers in ice sheets, Ann. Glaciol., 3, 195–198, 1982.

Mack, J. and Bolton, J. R.: Photochemistry of nitrite and nitrate in aqueous solution: a review, J. Photoch. Photobio. A, 128, 1–13, 1999.

Massucci, M., Clegg, S. L., and Brimblecombe, P.: Equilibrium partial pressures, thermodynamic properties of aqueous and solid phases, and Cl_2 production from aqueous HCl and HNO_3 and their mixtures, J. Phys. Chem. A, 103, 4209–4226, 1999.

McConnell, J. C., Henderson, G. S., Barrie, L., Bottenheim, J., Niki, H., Langford, C. H., and Templeton, E. M. J.: Photochem-

ical Bromine Production Implicated in Arctic Boundary-Layer Ozone Depletion, Nature, 355, 150–152, 1992.

McNeill, V. F., Loerting, T., Geiger, F. M., Trout, B. L., and Molina, M. J.: Hydrogen chloride-induced surface disordering on ice, P. Natl. Acad. Sci. USA, 103, 9422–9427, 2006.

McNeill, V. F., Geiger, F. M., and Loerting, T.: Interaction of hydrogen chloride with ice surfaces: The effects of grain size, surface roughness, and surface disorder, J. Phys. Chem. A, 111, 6274–6284, 2007.

Michalowski, B. A., Francisco, J. S., Li, S. M., Barrie, L. A., Bottenheim, J. W., and Shepson, P. B.: A computer model study of multiphase chemistry in the Arctic boundary layer during polar sunrise, J. Geophys. Res.-Atmos., 105, 15131–15145, 2000.

Molina, M. J., Tso, T. L., Molina, L. T., and Wang, F. C. Y.: Antarctic Stratospheric Chemistry of Chlorine Nitrate, Hydrogen Chloride and Ice – Release of Active Chlorine, Science, 238, 1253–1257, 1987.

Mulvaney, R., Wolff, E. W., and Oates, K.: Sulfuric-Acid at Grain-Boundaries in Antarctic Ice, Nature, 331, 247–249, 1988.

Rard, J. A., Clegg, S. L., and Platford, R. F.: Thermodynamics of {zNaCl+(1-z)Na_2SO_4}(aq) from T = 278.15 K to T = 318.15 K, and representation with an extended ion-interaction (Pitzer) model, J. Chem. Thermodyn., 35, 967–1008, 2003.

Rard, J. A., Wijesinghe, A. M., and Clegg, S. L.: Simplification of the Clegg-Pitzer-Brimblecombe Mole-Fraction Composition Based Model Equations for Binary Solutions, Conversion of the Margules Expansion Terms into a Virial Form, and Comparison with an Extended Ion-Interaction (Pitzer) Model, J. Solution Chem., 39, 1845–1864, 2010.

Robinson, C., Boxe, C. S., Guzman, M. I., Colussi, A. J., and Hoffmann, M. R.: Acidity of frozen electrolyte solutions, J. Phys. Chem. B, 110, 7613–7616, 2006.

Simpson, W. R., von Glasow, R., Riedel, K., Anderson, P., Ariya, P., Bottenheim, J., Burrows, J., Carpenter, L. J., Frieß, U., Goodsite, M. E., Heard, D., Hutterli, M., Jacobi, H.-W., Kaleschke, L., Neff, B., Plane, J., Platt, U., Richter, A., Roscoe, H., Sander, R., Shepson, P., Sodeau, J., Steffen, A., Wagner, T., and Wolff, E.: Halogens and their role in polar boundary-layer ozone depletion, Atmos. Chem. Phys., 7, 4375–4418, doi:10.5194/acp-7-4375-2007, 2007.

Solomon, S., Garcia, R. R., Rowland, F. S., and Wuebbles, D. J.: On the Depletion of Antarctic Ozone, Nature, 321, 755–758, 1986.

Takenaka, N. and Bandow, H.: Chemical kinetics of reactions in the unfrozen solution of ice, J. Phys. Chem. A, 111, 8780–8786, 2007.

Takenaka, N., Ueda, A., and Maeda, Y.: Acceleration of the Rate of Nitrite Oxidation by Freezing in Aqueous-Solution, Nature, 358, 736–738, 1992.

Takenaka, N., Ueda, A., Daimon, T., Bandow, H., Dohmaru, T., and Maeda, Y.: Acceleration mechanism of chemical reaction by freezing: The reaction of nitrous acid with dissolved oxygen, J. Phys. Chem., 100, 13874–13884, 1996.

Thibert, E. and Domine, F.: Thermodynamics and Kinetics of the Solid Solution of HCl in Ice, J. Phys. Chem. B, 101, 3554–3565, 1997.

Thibert, E. and Domine, F.: Thermodynamics and Kinetics of the Solid Solution of HNO_3 in Ice, J. Phys. Chem. B, 102, 4432–4439, 1998.

Thomas, J. L., Stutz, J., Lefer, B., Huey, L. G., Toyota, K., Dibb, J. E., and von Glasow, R.: Modeling chemistry in and above snow at Summit, Greenland – Part 1: Model description and results, Atmos. Chem. Phys., 11, 4899–4914, doi:10.5194/acp-11-4899-2011, 2011.

Tisdale, R. T., Prenni, A. J., Iraci, L. T., Tolbert, M. A., and Toon, O. B.: Variation of the infrared spectra of nitric acid hydrates with formation conditions: Impact on PSC identification, Geophys. Res. Lett., 26, 707–710, 1999.

Tolbert, M. A. and Middlebrook, A. M.: Fourier Transform Infrared Studies of Model Polar Stratospheric Cloud Surfaces: Growth and Evaporation of Ice and Nitric Acid/Ice, J. Geophys. Res., 95, 22423–22431, 1990.

Tong, C. H., Clegg, S. L., and Seinfeld, J. H.: Comparison of activity coefficient models for atmospheric aerosols containing mixtures of electrolytes, organics, and water, Atmos. Environ., 42, 5459–5482, 2008.

Voigt, C., Krcher, B., Schlager, H., Schiller, C., Krämer, M., de Reus, M., Vössing, H., Borrmann, S., and Mitev, V.: In-situ observations and modeling of small nitric acid-containing ice crystals, Atmos. Chem. Phys., 7, 3373–3383, doi:10.5194/acp-7-3373-2007, 2007.

von Kuhlmann, R. and Lawrence, M. G.: The impact of ice uptake of nitric acid on atmospheric chemistry, Atmos. Chem. Phys., 6, 225–235, doi:10.5194/acp-6-225-2006, 2006.

Wettlaufer, J. S.: Impurity Effects in the Premelting of Ice, Phys. Rev. Lett., 82, 2516–2519, 1999.

Wettlaufer, J. S., Worster, M. G., and Huppert, H. E.: The phase evolution of young sea ice, Geophys. Res. Lett., 24, 1251–1254, 1997.

Wexler, A. S. and Clegg, S. L.: Atmospheric aerosol models for systems including the ions H^+, NH_4^+, Na^+, SO_4^{2-}, NO_3,Cl, Br, and H_2O, J. Geophys. Res., 107, 4207, doi:10.1029/2001JD000451, 2002.

Wolff, E. W. and Paren, J. G.: A 2-Phase Model of Electrical-Conduction in Polar Ice Sheets, J. Geophys. Res., 89, 9433–9438, 1984.

Wolff, E. W., Mulvaney, R., and Oates, K.: Diffusion and Location of Hydrochloric-Acid in Ice – Implications for Polar Stratospheric Clouds and Ozone Depletion, Geophys. Res. Lett., 16, 487–490, 1989.